

## TITLE:

Enhancer architecture and chromatin accessibility constrain phenotypic space during development

## AUTHORS

Rafael Galupa<sup>1#</sup>, Gilberto Alvarez-Canales<sup>1\*</sup>, Noa Ottolie Borst<sup>1\*</sup>, Timothy Fuqua<sup>1\*</sup>, Lautaro Gandara<sup>1\*</sup>, Natalia Misunou<sup>1\*</sup>, Kerstin Richter<sup>1\*</sup>, Mariana R. P. Alves<sup>1</sup>, Esther Karumbi<sup>1</sup>, Melinda Liu Perkins<sup>1</sup>, Tin Kocjan<sup>1</sup>, Christine A. Rushlow<sup>2</sup> and Justin Crocker<sup>1#</sup>

\* Equal contribution, alphabetical order (last name)

# Correspondence: [rafael.galupa@embl.de](mailto:rafael.galupa@embl.de) and [justin.crocker@embl.de](mailto:justin.crocker@embl.de)

### Affiliations:

<sup>1</sup> European Molecular Biology Laboratory, 69117 Heidelberg, Germany

<sup>2</sup> Department of Biology, New York University, New York, NY 10003, USA

## QUOTE

“Chance and chance alone has a message for us.”

Milan Kundera, *The Unbearable Lightness of Being*

## ABSTRACT

Developmental enhancers are DNA sequences that when bound to transcription factors dictate specific patterns of gene expression during development. It has been proposed that the evolution of such cis-regulatory elements is a major source of adaptive evolution; however, the regulatory and evolutionary potential of such elements remains little understood, masked by selective constraints, drift and contingency. Here, using mutation libraries in *Drosophila melanogaster* embryos, we observed that most mutations in classical developmental enhancers led to changes in gene expression levels but rarely resulted in novel expression outside of the native cell- and tissue-types. In contrast, random sequences often acted as developmental enhancers, driving expression across a range of levels and cell-types, in patterns consistent with transcription factor motifs therein; random sequences including motifs for transcription factors with pioneer activity acted as enhancers even more frequently and resulting in higher levels of expression. Together, our findings suggest that the adaptive phenotypic landscapes of developmental enhancers are constrained by both enhancer architecture and chromatin accessibility. We propose that the evolution of existing enhancers is limited in its capacity to generate novel phenotypes, whereas the activity of *de novo* elements is a primary source of phenotypic novelty.

1 **MAIN TEXT**

2 Morphological changes generally result from changes in the spatiotemporal regulation of gene  
3 expression during development, and thus a major theory in evolutionary developmental biology  
4 proposes anatomical evolution to be based on the genetic and molecular mechanisms  
5 underlying the evolution of spatial gene regulation (Carroll, 2008). In line with this, the  
6 evolution of cis-regulatory elements, such as developmental enhancers (Jindal and Farley,  
7 2021), has been proposed to be a major component of phenotypical evolution across animals  
8 (Carroll, 2008; Koshikawa, 2015; Majic and Payne, 2020; Monteiro and Gupta, 2016; Nghe et  
9 al., 2020; Stern and Orgogozo, 2008). The so-called “cis-regulatory hypothesis” proposes that  
10 mutations in enhancers are a common and continuous source of morphological variation, and  
11 a means to escape the pleiotropic effects of mutations to protein coding regions (Carroll, 2008;  
12 Stern and Orgogozo, 2008). For instance, the evolution of wing pigmentation “spots” in  
13 *Drosophila* involved the gain of binding sites for different transcription factors in an enhancer  
14 controlling a pigmentation gene (Gompel et al., 2005), whereas the loss of pelvic structures in  
15 stickleback fish occurred via mutations that abrogate the activity of an enhancer controlling the  
16 homeobox gene *Pitx1* (Chan et al., 2010). Molecular mechanisms of cis-regulatory evolution  
17 have also been proposed to include duplications of existing enhancers, *de novo* emergence from  
18 existing non-regulatory DNA and co-option or exaptation of transposable elements or  
19 enhancers with unrelated activities (Emera et al., 2016; Erwin and Davidson, 2009; Fong and  
20 Capra, 2022; Indjeian et al., 2016; Koshikawa et al., 2015; Kvon et al., 2021; Long et al., 2016;  
21 Lynch et al., 2011; Rebeiz et al., 2011).

22 Despite elegant case studies, the extent to which these mechanisms contribute to the regulatory  
23 evolution of developmental enhancers remains an open question (Arnold et al., 2014; Smith et  
24 al., 2013). It is still unknown which changes in enhancer function are evolutionarily accessible,  
25 or how the distribution of transcription factor binding sites might constrain the evolutionary  
26 potential of enhancers (Fuqua et al., 2020). As such, there is a lack of clarity on the molecular  
27 genetic pathways for evolutionary change in animal development based on what is functionally  
28 possible *versus* what is probable and permissible from the standpoint of mutational events and  
29 natural selection (Carroll, 2008).

30 Here, we explored how molecular evolution of existing enhancers versus *de novo* sequences  
31 contributes to producing novel patterns of gene expression across *Drosophila melanogaster*  
32 embryos. We generated and characterized a panel of unbiased mutation libraries for both  
33 classical developmental enhancers and randomly generated sequences; this approach allows to  
34 distinguish constraints that emerge from the prior function or evolutionary histories of existing  
35 enhancers from constraints that arise from properties of the sequence or locus unrelated to  
36 selection processes.

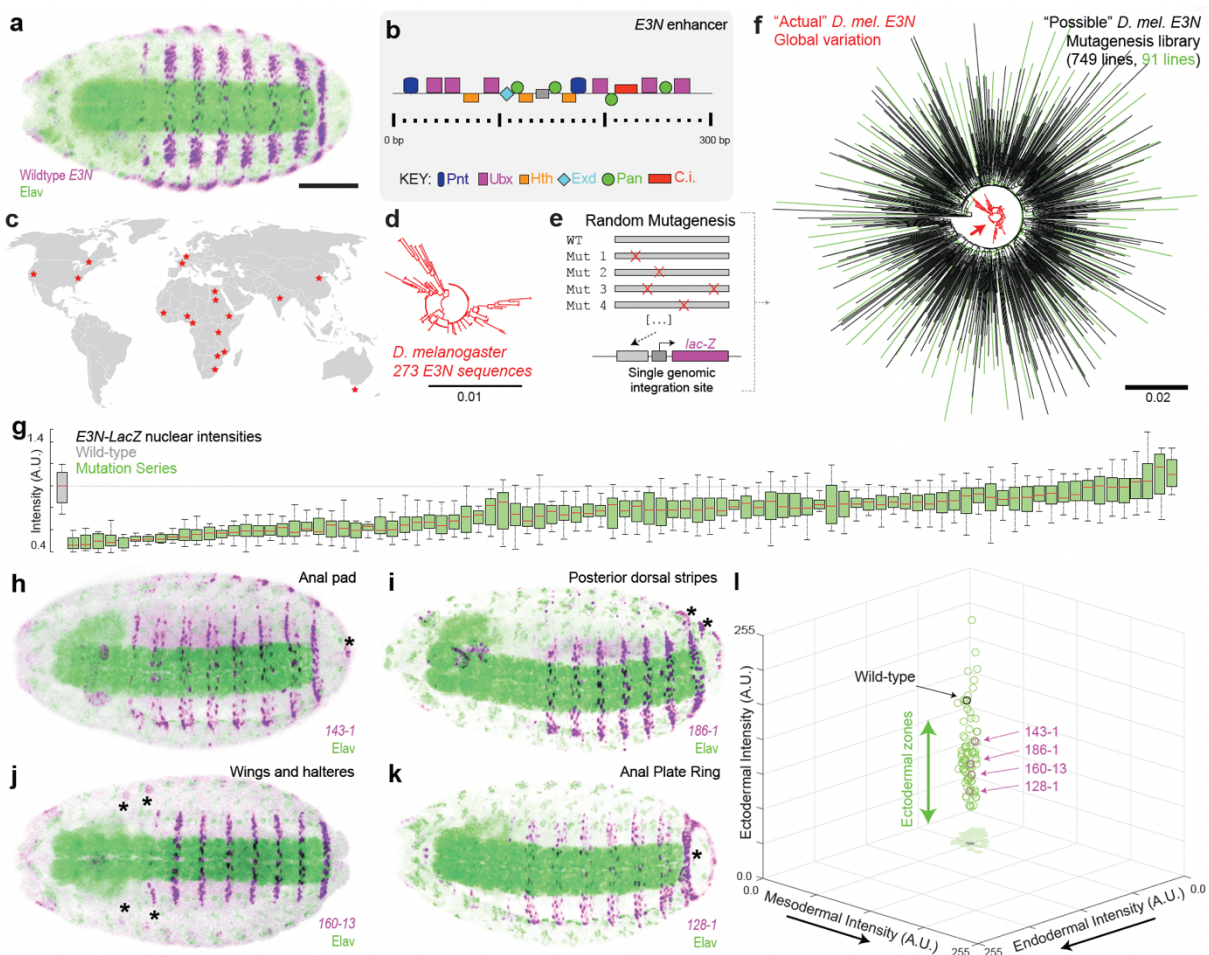
37 **Constrained capacity for enhancer-driven expression outside of native expression  
38 patterns**

39 We first set out to investigate whether and how mutations across developmental enhancers  
40 could lead to ectopic, novel expression patterns. We have previously generated a mutation  
41 library for the *E3N* enhancer, which regulates the expression of *shavenbaby* (**Fig. 1A-B**) (Fuqua  
42 et al., 2020). This mutation library included 749 variants and most mutations led to changes in

43 transcriptional outputs (e.g., levels, location) (Fuqua et al., 2020). This library represents a ~6  
 44 times larger sequence space than the natural variation found for *D. melanogaster* *E3N* from  
 45 samples across the world (Fig. 1C-F, Fig. S1). To investigate novel expression patterns, we  
 46 selected a subset of lines harboring 1-10 point mutations for further characterization; these lines  
 47 come from different regions of the sequence space covered by the total library (Fig. 1F; Table  
 48 S1) and showed a spectrum of effects in terms of expression levels (Fig. 1G). We found that  
 49 22% of the lines showed expression outside of the usual *E3N*-driven ventral stripes, in regions  
 50 such as prospective anal pads, wing and haltere imaginal discs and other structures (Fig. 1H-  
 51 K). However, these regions are ectoderm-derived and correspond to regions where the target  
 52 gene of *E3N* (*svb*) is expressed (Frankel et al., 2010; Preger-Ben Noon et al., 2018).

53 To evaluate ectopic expression across regions derived from different germ layers, we quantified  
 54 reporter-expression intensity in the selected lines (Fig. S2) and detected no expression in  
 55 regions derived from germ layers other than the ectoderm (Fig. 1L), whereas variable levels of  
 56 expression along the “ectoderm” axis could be seen (Fig. 1L). These results suggest that  
 57 evolving new patterns of expression upon point mutations of a developmental enhancer is  
 58 possible but developmentally biased to specific lineages.

59



60

61 **Figure 1: Mutant variants of the *E3N* enhancer have a limited capacity for expression**  
 62 **outside native tissues- and cell-types. (A)** Pattern of expression driven by wildtype *E3N* at

63 stage 15 (beta-galactosidase protein staining). Scale bar 100  $\mu$ m. **(B)** Mapped binding site  
64 architecture for *E3N*. **(C)** Collection locations of sequenced *Drosophila melanogaster* strains  
65 (Lack et al., 2016). **(D)** Phylogenetic tree of *E3N* sequences across *D. melanogaster* strains.  
66 **(E)** Schematic of enhancer variants and reporter gene construct used for integration into the *D.*  
67 *melanogaster* genome. **(F)** Phylogenetic tree of *E3N* sequences across *D. melanogaster* strains  
68 (red) and of *E3N* sequences from our mutational library (black and green; in green, 91 lines  
69 selected for further characterization). **(G)** Nuclear intensities of the A2 segment across 91 lines,  
70 normalized to wildtype *E3N* (n=10 embryos per line). A.U., arbitrary units of fluorescence  
71 intensity. **(H-K)** Examples of mutant variants leading to reporter expression outside the  
72 wildtype *E3N* pattern. In panels (h) and (i), expression associated to esophagus is likely an  
73 artifact of the construct used, as observed in other lines unrelated to *E3N*. **(L)** 3D plot showing  
74 fluorescence intensities for 91 lines across three regions of the embryo with different germ-  
75 layer origins (see Fig. S2). Each dot corresponds to the average value for one variant enhancer  
76 line.

77

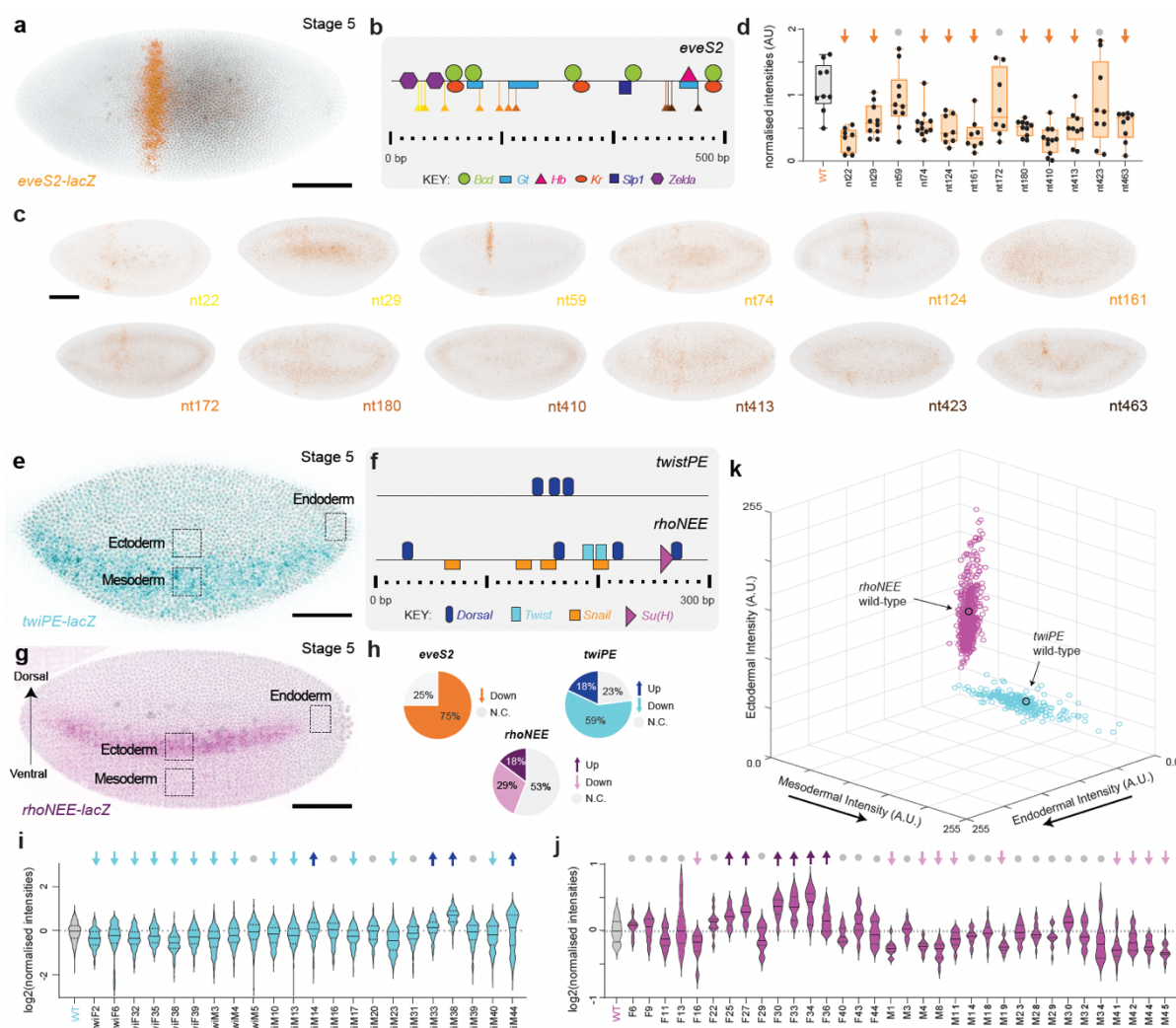
## 78 **The emergence of ectopic expression patterns upon mutagenesis of developmental 79 enhancers is rare**

80 To explore whether the transcriptional constraints we observed for *E3N* mutagenesis are a  
81 general property of developmental enhancers, and given that *E3N* regulates a terminal selector  
82 gene in later development (Allan and Thor, 2015), we chose to explore additional “classical”  
83 enhancers involved in early development. These include *eveS2*, important for anterior-posterior  
84 specification (**Fig. 2A-B**), (Small et al., 1991, 1992; Stanojevic et al., 1991), and *rhoNEE* and  
85 *twiPE*, both involved in dorsoventral patterning (**Fig. 2E-G**), in the neurogenic ectoderm and  
86 mesoderm, respectively (Bier et al., 1990; Ip et al., 1992; Jiang et al., 1991; Markstein et al.,  
87 2004; Pan et al., 1991; Thisse et al., 1991). For each of these enhancers, we generated mutant  
88 libraries using the same setup as for the *E3N* library (Fuqua et al., 2020): each variant was  
89 cloned upstream of a heterologous *hsp70* promoter driving *lacZ* reporter expression and  
90 integrated into the *Drosophila* genome at a specific landing site, amenable to expression across  
91 different tissues and stages (**Fig. S1**). Using a PCR error-rate of ~0.5% per molecule, we  
92 isolated enhancer variants containing approximately 1-5 mutations in 12-36 independent fly  
93 lines per enhancer (Table S1).

94 We examined reporter activity across all lines in the early embryo (stage 5) and found similar  
95 trends for all of them. On the one hand, mutations often led to significant changes in expression  
96 levels, and on the other hand, changes in expression were restricted to the native pattern – no  
97 ectopic expression was observed. For *eveS2* (**Fig. 2A**), each variant contained a single mutation  
98 only, almost none overlapping a known binding site (**Fig. 2B-C**). Yet, 75% led to significantly  
99 reduced expression compared to control (**Fig. 2D, 2H**), suggesting that it is relatively easy to  
100 “break” the minimal *eveS2* enhancer, consistent with unsuccessful attempts to build this  
101 enhancer *de novo* (Crocker and Ilsley, 2017; Vincent et al., 2016). In no case did we observe  
102 expression outside of the *eve* stripe 2 region. Similar results were found for *rhoNEE* and *twiPE*:  
103 47% and 77% of enhancer variants, respectively, showed statistically significant changes in  
104 nuclear intensities compared to control (**Fig. 2H**); for *rhoNEE*, 18% showed higher expression

105 and 29% showed lower expression (**Fig. 2J**); for *twiPE*, these values were 18% and 59%  
 106 respectively (**Fig. 2I**). These effects did not seem to correlate with the number of mutations per  
 107 enhancer (**Fig. S3**) nor with the length of the enhancer (compare Fig. 2b and 2f with 2h). Again,  
 108 despite clear changes in levels for most mutant variants, we noted that expression outside of  
 109 the typical area of expression for each enhancer was never observed – quantification of  
 110 expression in control and mutant lines across regions of the embryo that will give rise to  
 111 ectoderm (lateral region of the embryo), endoderm (posterior region of the embryo) and  
 112 mesoderm (ventral region of the embryo; regions highlighted in **Fig. 2E, 2G**) revealed that  
 113 mutant lines showed changed levels of expression but always within the “ectoderm” and  
 114 “mesoderm” regions only, for *rhoNEE* and *twiPE* enhancers respectively (**Fig. 2K**). In  
 115 summary, most mutations led to changes in expression levels within native zones of expression;  
 116 thus, the results suggest that the “molecular evolution” by point mutations of developmental  
 117 enhancers is not likely to result in novel expression patterns.

118



119

120 **Figure 2: Mutagenesis across early developmental enhancers alters gene expression only**  
 121 **within native patterns of expression. (A)** Pattern of expression driven by wildtype *eveS2* at  
 122 stage 5 (lacZ mRNA staining). Scale bar 100 μm. **(B)** Known binding site architecture for  
 123 *eveS2*. Location of point mutations is indicated. **(C)** Examples of stained embryos from

124 different *eveS2* single-nucleotide mutant variants. The name of each line corresponds to the  
125 location of the point mutation (compare with **B**). **(D)** Fluorescence intensities of the region  
126 where the wildtype *eveS2* shows a stripe across 12 single-nucleotide *eveS2* variants (n=8-11  
127 embryos per line). Lines marked with an arrow are statistically significantly different from  
128 wildtype ( $p<0.05$ ; two-tailed t-test). A.U., arbitrary units of fluorescence intensity. **(E)** Pattern  
129 of expression driven by wildtype *twiPE* at stage 5 (lacZ mRNA staining). **(F)** Known binding  
130 site architecture for *twiPE* and *rhoNEE*. **(G)** Pattern of expression driven by wildtype *rhoNEE*  
131 at stage 5 (lacZ mRNA staining). **(H)** Summary of changes in expression levels for the *eveS2*,  
132 *twiPE* and *rhoNEE* lines. **(I-J)** Nuclear intensities across *twiPE* (**I**) and *rhoNEE* (**J**) variants  
133 (n=6-27 embryos per line). Lines marked with an arrow (up or down) are statistically  
134 significant from wildtype ( $p<0.05$ ; two-tailed t-test). **(K)** 3D plot showing fluorescence  
135 intensities for *twiPE* (blue) and *rhoNEE* (purple) lines across three regions of the embryo  
136 illustrated in **(I)** and **(J)**. Each dot corresponds to one embryo; three embryos per line were  
137 quantified.

138

---

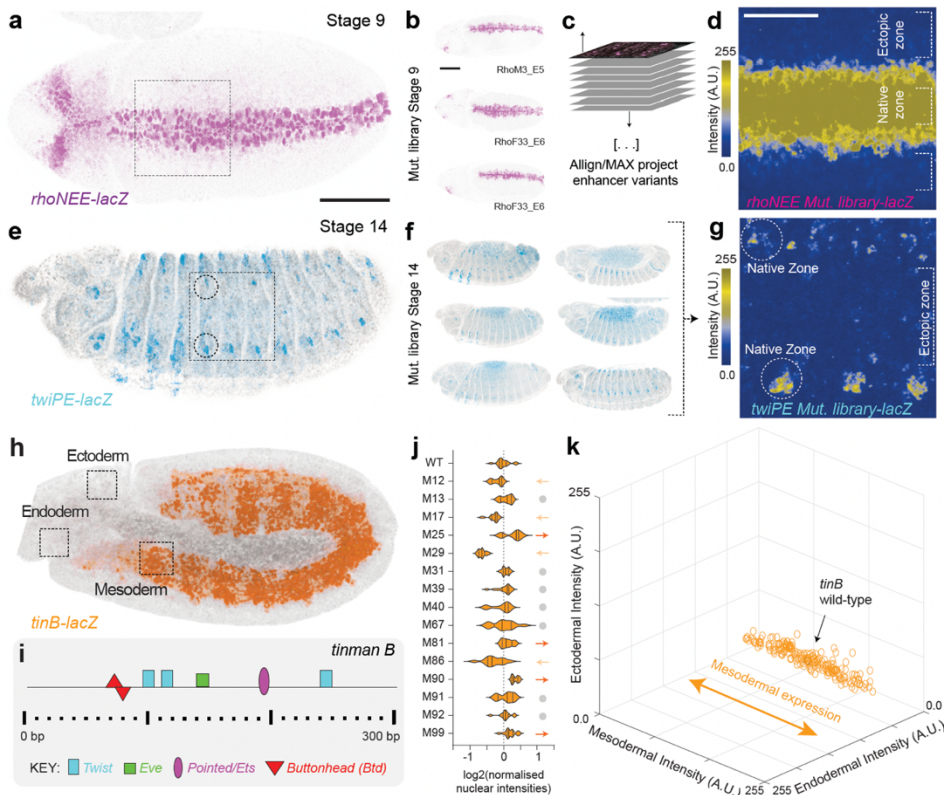
139

140 Considering that such pleiotropic effects could be revealed throughout development (Preger-  
141 Ben Noon et al., 2018), we analyzed expression in embryos at later stages (stage 9 and 14) for  
142 the *rhoNEE* (**Fig. 3A**; **Fig. S4**) and *twiPE* libraries (**Fig. 3E**; **Fig. S5**) but we observed no  
143 ectopic expression in the mutant lines compared to the control (**Fig. 3B-D, 3F-G**). We also  
144 generated an additional mutational library for *tinB*, an enhancer that controls a mesoderm-  
145 specific gene throughout a broad developmental window (**Fig. 3H-I**; Table S1) (Yin et al.,  
146 1997; Zaffran et al., 2006). Similar to what we found for early enhancers, 47% of enhancer  
147 variants showed significant changes in enhancer activity (**Fig. 3J**; 20% showed increased  
148 expression, 27% showed decreased expression), yet no ectopic expression was observed (**Fig.**  
149 **3K**).

150 Finally, we tested whether ectopic expression could be “forced” upon recruitment of a  
151 ubiquitously expressed synthetic transcription factor. The *rhoNEE* enhancer has been  
152 previously engineered to contain binding sites for a transcription activator-like effector (TALE)  
153 DNA-binding protein (Crocker et al., 2016). We crossed fly lines harboring *rhoNEE* enhancers  
154 with one, two or three TALE binding sites with a line containing a TALE protein fused to the  
155 strong activation domain VP64 (Beerli et al., 1998) and expressed via a nos::Gal4 driver, and  
156 quantified expression across different regions of the early embryo (**Fig. S7**). The higher the  
157 number of binding sites for the synthetic transcription factor, the higher the expression within  
158 the usual regions of *rhoNEE* expression. However, it was not until there were two or more  
159 binding sites (16bp long) that appreciable expression was generated outside of the native zones  
160 of expression (**Fig. S7**). Together, these results reveal that the *rhoNEE* enhancer is not  
161 ‘intrinsically’ refractory to expression outside of its usual pattern of expression, but rather  
162 requires a considerably larger recruitment of activators to the locus. The fact that we do not  
163 observe ectopic expression in the enhancer libraries analyzed suggests that regulatory  
164 constraints are imposed on developmental enhancers.

165

166



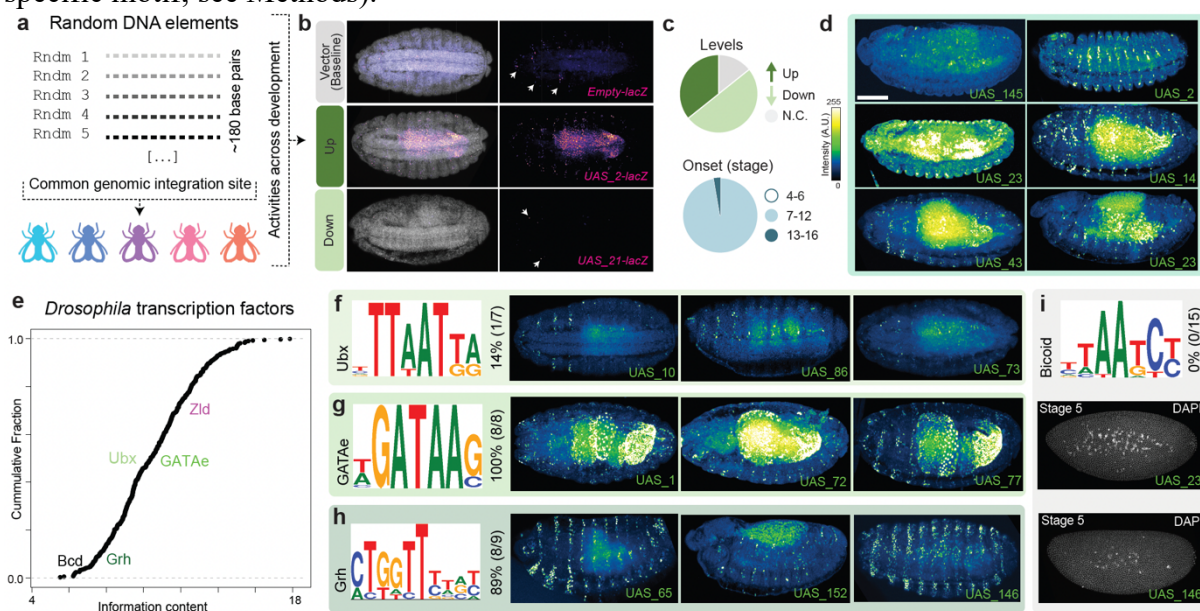
167

168 **Figure 3: Mutagenesis across late developmental enhancers alters gene expression only**  
169 **within native patterns of expression. (A)** Pattern of expression driven by wildtype *rhoNEE*  
170 at stage 9 (beta-galactosidase protein staining). Scale bar 100  $\mu$ m. **(B)** Examples of stained  
171 embryos from different *rhoNEE* mutant variants. Scale bar 100  $\mu$ m. **(C)** Schematic of  
172 alignment and overlaying of individual Z-projections of maximum intensity for *rhoNEE* mutant  
173 variants. **(D)** Heatmap of aggregated Z-projections. Scale bar 50  $\mu$ m. **(E)** Pattern of expression  
174 driven by wildtype *twiPE* at stage 14 (beta-galactosidase protein staining). **(F)** Examples of  
175 stained embryos from different *twiPE* mutant variants. **(G)** Heatmap of aggregated Z-  
176 projections upon alignment of individual Z-projections of maximum intensity for *twiPE* mutant  
177 variants. **(H)** Pattern of expression driven by wildtype *tinB* at stage 10 (beta-galactosidase  
178 protein staining). **(I)** Known binding site architecture for *tinB*. **(J)** Nuclear intensities across  
179 *tinB* variants (n=10-18 embryos per line). Lines marked with an arrow (up or down) are  
180 statistically significant from wildtype ( $p < 0.05$ ; two-tailed t-test). **(K)** 3D plot showing  
181 fluorescence intensities for *tinB* lines across three regions of the embryo as illustrated in (H).  
182 Each dot corresponds to one embryo; at least ten embryos per line were quantified.

183 **Random sequences lead to extensive expression across developmental time and space**

184 We interrogated the extent to which *de novo* sequences, devoid of evolutionary constraints,  
185 could act as enhancers and drive expression across the embryo and across development. We  
186 synthesized random sequences (~180bp), inserted them upstream of *hsp70* promoter driving  
187 *lacZ* (similarly to the enhancer libraries) and integrated them into the fly genome at the same  
188 genomic location (Fig. 4A, Fig. S8). These sequences included a motif (UAS) for the yeast

189 Gal4 transcription factor (Kakidani and Ptashne, 1988; Webster et al., 1988), which is not  
 190 present in the fly and thus this motif should be “neutral”; this design was chosen so that these  
 191 sequences have a comparable architecture to libraries containing other motifs (see later). We  
 192 isolated 56 fly lines harboring unique sequences (Table S1), for which we stained embryos at  
 193 different stages to determine reporter gene’s expression pattern(s). Surprisingly, 86% of  
 194 sequences led to changes in reporter expression at least in some cells and/or at some  
 195 developmental stage, compared to expression of the reporter with no sequence cloned upstream  
 196 (**Fig. 4B-D**; **Fig. S9**). The other surprising observation was that despite such pervasive  
 197 expression, we never observed expression in the early embryo (**Fig. 4C**). Given the variable  
 198 consensus sites found in multicellular systems, such libraries are expected to have a range of  
 199 motifs with variable information content (de Boer et al., 2019; Wunderlich and Mirny, 2009)  
 200 (**Fig. 4E**). To explore the expression patterns observed, we conducted motif searches across all  
 201 random sequences for *Drosophila* developmental transcription factors (**Fig. 4E**; Methods).  
 202 Motifs found included Ultrabithorax (Ubx), GATA, Gravyhead (Grh) and Bicoid (Bcd) motifs  
 203 (**Fig. 4F-I**). Interestingly, 100% or 80% of the random DNA elements containing, respectively,  
 204 a GATA or Grh motif showed expression (**Fig. 4G-H**), consistent with their previously  
 205 reported predictive power (de Almeida et al., 2022; Kvon et al., 2014) and with the expression  
 206 patterns of the respective transcription factors. In contrast, only 14% of elements with a Ubx  
 207 motif showed expression (**Fig. 4F**) and none of the elements containing a Bcd motif showed  
 208 expression (**Fig. 4I**), consistent with the absence of expression in the early embryo for all  
 209 random sequences. We calculated whether our random sequences were biased for motifs of  
 210 late-development transcription factors (TFs), but this did not explain the absence of early  
 211 expression (average per sequence: ~3.9 hits per early-specific motif *versus* ~3.4 hits per late-  
 212 specific motif; see Methods).



213

214 **Figure 4: Random DNA sequences often drive reporter expression during development.**  
 215 (A) Schematic of the UAS-library. (B) Expression patterns at stage 15 were compared to the  
 216 reporter with no sequence cloned upstream (top) and classified as “up” (middle) or “down”  
 217 (bottom), depending on whether expression was increased or decreased, respectively. (C)

218 Summary of changes in expression levels at stage 15 (top) based on panel **(B)**, and of  
219 developmental period in which expression is first observed (bottom). **(D)** Examples of stained  
220 embryos from different random DNA sequences. **(E)** Cumulative distribution function of the  
221 expected frequency of *Drosophila* TF motifs in random DNA. **(F)** Ubx motif, percentage of  
222 lines showing expression among random DNA lines with a Ubx motif and examples of  
223 corresponding embryos. **(G)** GATA motif, percentage of lines showing expression among  
224 random DNA lines with a GATA motif and examples of corresponding embryos. **(H)** Grh  
225 motif, percentage of lines showing expression among random DNA lines with a Grh motif and  
226 examples of corresponding embryos. **(I)** Bicoid motif, percentage of lines showing expression  
227 among random DNA lines with a Bcd motif and examples of corresponding embryos.

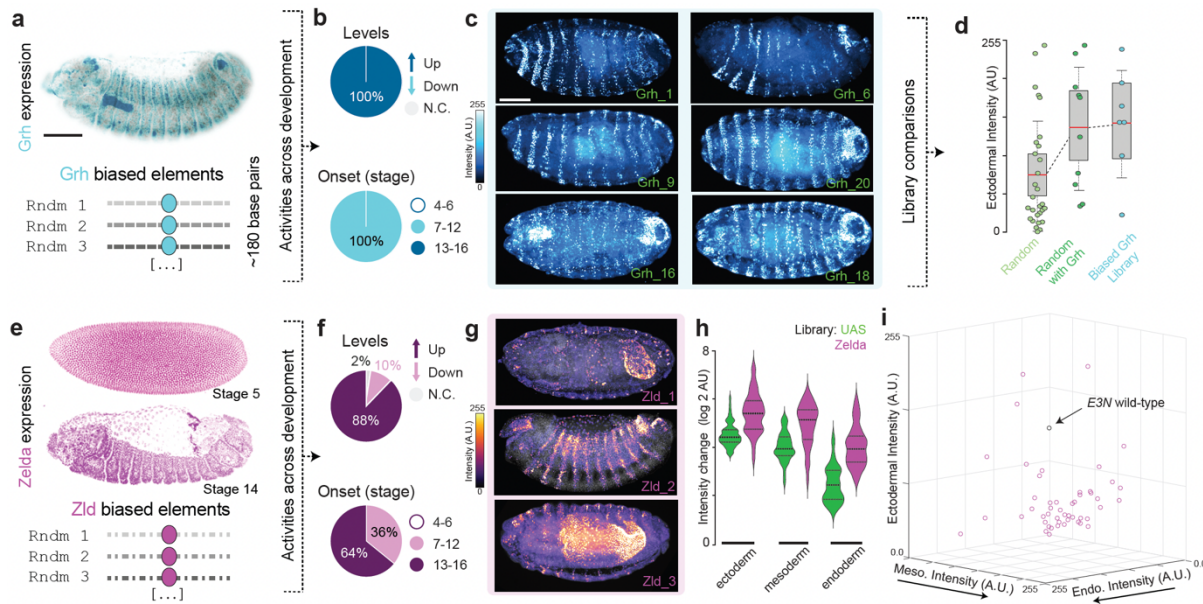
228

## 229 **Specific motifs can potentiate emergence of enhancer activity**

230 Completely random sequences thus seem to have a high potential of driving expression, and  
231 this can be associated to particular motifs. Given the association between chromatin  
232 accessibility and transcriptional permissiveness (Klemm et al., 2019), as well as studies  
233 suggesting that chromatin accessibility might underlie enhancer evolution (Peng et al., 2019;  
234 Xin et al., 2020), we generated “biased” random libraries in which we included a Grh motif  
235 (**Fig. 5A**; 7 lines, Table S1) or a Zelda motif (**Fig. 5E**; 41 lines, Table S1) approximately at the  
236 center of random sequences. Grainyhead and Zelda are transcription factors in the fly reported  
237 to have “pioneer activity” (Hansen et al., 2022; Zaret and Carroll, 2011) – their binding is  
238 associated with “opening” chromatin, rendering enhancers more accessible to binding by other  
239 transcription factors (Foo et al., 2014; Harrison et al., 2011; Iwafuchi-Doi, 2019; Jacobs et al.,  
240 2018; Larson et al., 2021; Nevil et al., 2020; Schulz et al., 2015; Sun et al., 2015). Though  
241 Zelda is usually associated with early fly development, it is expressed throughout development  
242 (**Fig. S10**) and its late embryonic knockout has phenotypical consequences (**Fig. S11**).  
243 Consistent with the idea of “pioneer activity”, an even higher proportion of random sequences  
244 from the Grh and Zld “biased” libraries drove expression compared to the UAS library (**Fig.**  
245 **5B-C, 5F-G; Fig. S12**). Not only a higher number of lines was associated with expression for  
246 the “biased” libraries, but also expression levels were higher when compared to the UAS-  
247 library, regardless of the region of the embryo (**Fig. 5D, 5H-I**). To further test the potential of  
248 these motifs, we added one or two Zelda motifs to the developmental enhancers we tested  
249 initially (*eveS2*, *rhoNEE*, *twiPE*, *tinB*) and found a significant increase in reporter expression  
250 levels for all enhancers within their native patterns of expression (**Fig. S13**). For the *eveS2*  
251 lines, we additionally observed novel, ectopic expression (**Fig. S13**), suggesting that the Zelda  
252 motifs might “unlock” cryptic sites contained in *eveS2*. We tested whether *eveS2* contained  
253 more predicted motifs than the other enhancers, but we did not find any significant differences  
254 in the number of hits (0.07 for *eveS2* versus 0.10, 0.12 and 0.05 for *rhoNEE*, *tinB* and *twiPE*,  
255 respectively; normalized per enhancer length).

256 To explore the possibility that the occurrence of specific motifs throughout the genome might  
257 contribute to the emergence of (*de novo*) enhancers, we selected genomic sequences containing  
258 high-affinity Ubx/Hth motifs (ATGATTATGAC) (Slattery et al., 2011) present in *D. melanogaster*  
259 but not in other *Drosophila* species (**Fig. S14**). Such motifs have been

260 demonstrated to augment chromatin accessibility (Loker et al., 2021) and are broadly used  
261 across development, providing a counterpoint to our synthetic libraries. Strikingly, when we  
262 tested their enhancer potential with the *lacZ* reporter assay, all sequences showed enhancer  
263 activity (Fig. S14). Mutating the *Ubx/Hth* motif in each of those sequences led to a dramatic  
264 reduction in expression for six out of seven of those sequences (Fig. S14), indicating that these  
265 motifs clearly have the capacity to drive expression across development. These results support  
266 the idea that specific sequence motifs might prime genomic sequences to act and/or evolve as  
267 enhancers.



268 **Figure 5: Specific DNA motifs enhance likelihood of reporter expression during**  
269 **development. (A)** Staining for Grh transcription factor (top) and schematic of the Grh-library  
270 (bottom). **(B)** Summary of changes in expression levels (top) compared to the reporter with no  
271 sequence cloned upstream (Fig. S9) and of developmental period in which expression is first  
272 observed (bottom). **(C)** Examples of stained embryos from different Grh-biased sequences. **(D)**  
273 Quantification of fluorescent intensities in ectoderm-associated region for all random DNA  
274 sequences, for random DNA sequences with Grh motifs (subset of all random DNA sequences)  
275 and for Grh-biased sequences. **(E)** Staining for Zld transcription factor (top) and schematic of the  
276 Zld-library (bottom). **(F)** Summary of changes in expression levels at stage 15 (top) compared to the  
277 reporter with no sequence cloned upstream (Fig. S9) and of developmental period in which expression is  
278 first observed (bottom). **(G)** Examples of stained embryos from different Zld-biased sequences. **(H)**  
279 Quantification of fluorescent intensities for Zld-biased lines across three regions of the embryo (see Fig. S2). **(I)**  
280 3D plot showing fluorescence intensities for Zld-biased lines, based on (H). Each dot corresponds to one line. For reference,  
281 fluorescence intensity for the wildtype *E3N* sequence is shown (from Fig. 1L).

284  
285 **DISCUSSION**  
286 We used transgenesis-based mutagenesis and *de novo* gene synthesis during fly embryogenesis  
287 to investigate evolutionary pathways for enhancer activity. We used fly development to explore

288 how novel patterns of gene expression might appear from either “molecular evolution” of  
289 developmental enhancers or random sequences. Notably, while reporter gene assays and  
290 minimal enhancers may not reflect the full regulatory activities of native loci (Halfon, 2019;  
291 Lindhorst and Halfon, 2022; López-Rivera et al., 2020), such an approach allows us to evaluate  
292 a broad range of “possible” enhancer variation in a controlled experimental setup, without  
293 associated fitness costs and allowing a broader exploration of evolution and development  
294 without the complexities and historical contingencies found in nature. Furthermore, using such  
295 an assay in a developmental model system, which generates an embryo in 24 hours, we can  
296 assay regulatory activities across ~100,000 cells of different lineage origins (Song et al., 2019).

297 Using this approach, we found that most mutations in enhancers led to changes in levels of  
298 reporter gene expression, but almost entirely within their native zones of expression (**Figs. 1-**  
299 **3**), similar to previous studies using transgenic mutagenesis of the *Shh* enhancer in murine  
300 embryos (Kvon et al., 2020), or the *E3N* enhancer (Fuqua et al., 2020) and the wing spot<sup>196</sup>  
301 enhancer (Le Poul et al., 2020) in fly embryos. Consistent with our results, known phenotypic  
302 evolution through nucleotide mutations of standing regulatory elements seems to appear either  
303 through changes in the levels or timings of expression within native zones or the loss of  
304 regulatory activities. For example, the evolution of pigmentation spots in fly wings occurred  
305 via a specific spatial increase in the melanic protein Yellow, which is uniformly expressed at  
306 low levels throughout the developing wings of fruit flies (Gompel et al., 2005); see (Frankel et  
307 al., 2011; Rebeiz et al., 2009) for other examples of evolution within native patterns of  
308 expression. Evolution of other traits such as thoracic ribs in vertebrates (Guerreiro et al., 2013),  
309 limbs in snakes (Kvon et al., 2016), pelvic structures in sticklebacks (Chan et al., 2010) and  
310 seed shattering in rice (Konishi et al., 2006) are all associated with loss of enhancer activity  
311 due to internal enhancer mutations. Additionally, mutations have been found to occur less often  
312 in functionally constrained regions of the genome, suggesting that mutation bias may reduce  
313 the occurrence of deleterious mutations in regulatory regions (Monroe et al., 2022).

314 Consistent with these results, phenotypic novelties underlain by enhancer-associated ectopic  
315 gains of expression are reportedly due to transposon mobilisation (Bourque et al., 2008; Emera  
316 and Wagner, 2012; Feschotte, 2008; Oliver and Greene, 2009), rearrangements in chromosome  
317 topology (Galupa and Heard, 2017; Gilbertson et al., 2022; Lupiáñez et al., 2016) or *de novo*  
318 evolution of enhancers from DNA sequences with unrelated or nonregulatory activities (Arnold  
319 et al., 2014; Birnbaum et al., 2012; Eichenlaub and Ettwiller, 2011; Emera et al., 2016; Li et  
320 al., 2022; Prabhakar et al., 2008; Rebeiz et al., 2011). Previous studies have explored the  
321 potential of random DNA sequences to lead to reporter gene expression, either as enhancers or  
322 promoters, especially in cell lines of prokaryotic or eukaryotic origin (de Almeida et al., 2022;  
323 Vaishnav et al., 2022; Yona et al., 2018). These have shown that there is a short (or sometimes  
324 null) mutational distance between random sequences and active *cis*-regulatory elements (Yona  
325 et al., 2018), which may improve evolvability. In our study, we tested random sequences in a  
326 developmental context and found that most showed enhancer activity across several types of  
327 tissues and developmental stages (**Fig. 4**). These results are consistent with a study that tested  
328 enhancer activity of all 6-mers in developing zebrafish embryos and found a diverse range of  
329 expression for ~38% of the sequences at two developmental stages (Smith et al., 2013). We  
330 observed expression driven by random sequences even in the absence of motifs within their

331 sequence for transcription factors with pioneering activity (**Fig. 4**). Yet, when such motifs were  
332 included, nearly all sequences acted as “strong” enhancers (leading to high levels of expression)  
333 (**Fig. 5**), consistent with the “evolutionary barrier” to the formation of a novel enhancer being  
334 lower in regions that already contain motifs for DNA binding factors, which can “act  
335 cooperatively with newly emerging sites” (Long et al., 2016).

336 It is interesting to note that, despite the high potential of random sequences to be expressed  
337 during development and across cell types, we never observed expression prior to gastrulation;  
338 this was not evaluated in the zebrafish study or in other studies. This may be due to the rapid  
339 rates of early fruit fly development, in which gene expression patterns are highly dynamic, and  
340 cell-fate specifications occur within minutes (Surkova et al., 2018). As such, there may be  
341 extensive regulatory demands placed on transcriptional enhancers, reflected in the clusters of  
342 high-affinity binding sites common across early embryonic developmental enhancers (Crocker  
343 et al., 2015) as well as their extensive conservation in function (Hare et al., 2008) and location  
344 (Cande et al., 2009). In the future, it will be interesting to explore how regulatory demands that  
345 change across development – such as nuclear differentiation, network cross-talk, and metabolic  
346 changes – are reflected in regulatory architectures and their evolvability.

347 The observation that most random sequences led to expression suggests that the potential of  
348 any sequence within the genome to drive expression is enormous and thus “an important  
349 playground for creating new regulatory variability and evolutionary innovation” (Eichenlaub  
350 and Ettwiller, 2011). This was further supported by the regulatory potential of the genomic  
351 sequences we tested, containing Ubx/Hth motifs. Perhaps the challenge from an evolutionary  
352 perspective has not been what allows expression, but what prevents expression; thus,  
353 mechanisms that repress “spurious” expression might have evolved across genomes. This is in  
354 line with propositions that nucleosomal DNA in eukaryotes has evolved to repress transcription  
355 (Muers, 2013; Wade and Grainger, 2018), along with transcriptional repressors and other  
356 mechanisms such as DNA methylation, as a response (at least partially) to “the unbearable ease  
357 of expression” present in prokaryotes (Gophna, 2018). The action of such repressive  
358 mechanisms could also explain why mutagenesis of developmental enhancers, which are  
359 subject to evolutionary selection, does not easily lead to expression outside their native patterns  
360 of expression. In sum, our findings raise exciting questions about the evolution of enhancers  
361 and the emergence of novel patterns of expression that may underlie new phenotypes,  
362 suggesting an underappreciated role for *de novo* evolution of enhancers by happenstance.  
363 Genetic theories of morphological evolution will benefit from comparing controlled, multi-  
364 dimensional laboratory experiments with standing variation (Laland et al., 2015); such an  
365 integrative approach could provide the frameworks that will enable us to make both  
366 transcriptional and evolutionary predictions.

## METHODS

### Fly strains and constructs

All mutant and random enhancer sequences were synthesized and cloned (GenScript) into pLacZattB plasmid at HindIII/XbaI site. *E3N*- and *eveS2*-related lines were injected into attP2

line, all other constructs were injected into VK33 line; injections done by Genetivision. Transgenic lines were homozygosed and genotyped; sequences are listed in Table S1.

#### Embryos collection and fixation

Flies were loaded into egg collection chambers, left to acclimatize for 3-4 days and then embryos were collected for either four or sixteen hours, for early and late stages, respectively. Embryos were dechorionated in 5% bleach for 2min, abundantly rinsed with water and washed in a saline solution (0.1 M NaCl and 0.04% Triton X-100), before transfer to scintillation vials containing fixative solution (700  $\mu$ l 16% PFA, 1.7 ml PBS/EGTA, 3.0 ml 100% heptane). Embryos were fixed for 25 min, shaking at 250 rpm. The lower phase was then removed, 4.6 mL 100% methanol added and vials vortexed at maximum speed for 1min. The interphase and upper phase were removed and the embryos were washed thrice in fresh methanol. Embryos were stored at -20 °C until processed.

#### Reporter gene expression analysis

*In situ hybridization (probes):* probes for *lacZ* (reporter) and *snail* (internal control) were generated from PCR products using the in vitro transcription (IVT) kit from Roche (#11175025910) and following manufacturer's instructions. A list of primer sequences for each PCR product can be found in Table S1. For each gene, distinct PCR products were pooled before IVT reaction. Probes were diluted in hybridization buffer (Hyb; 50% formamide, 4X SSC, 100  $\mu$ g/mL salmon DNA, 50  $\mu$ g/mL heparin, 0.1% Tween-20) at 50ng/ $\mu$ L. Prior to hybridization, a probe solution was prepared (per sample, 50 ng of each probe in 100  $\mu$ L), denatured at 80 °C for 5min, then immediately put on ice for 5min, and finally incubated at 56 °C for 10min before added to the embryos.

*In situ hybridization (procedure):* embryos stored in methanol were washed in methanol/ethanol (50:50), three-times in 100% ethanol and then permeabilized in xylenes (90% in ethanol) for 1h, after which embryos were washed six times in ethanol and three times in methanol. Embryos were then washed three times in PBT (PBS + 0.1% Tween-20) before post-fixation for 25min in fixative solution (225  $\mu$ l 16% PFA, 500  $\mu$ l PBT). Embryos were then washed several times in PBT for 40 min, followed by a wash in PBT/Hyb (50:50) at room temperature and a 30min-wash in pre-warmed Hyb at 56 °C. Embryos were then incubated with probe solution at 56°C overnight. The next day, embryos were washed in Hyb (three quick washes followed by three 30-min washes), then in Hyb/PBT (50:50), then in PBT several times for one hour before incubated for 30 min in blocking solution (Roche #11921673001; diluted 1:5 in PBT). Embryos were then incubated in blocking + primary antibodies diluted 1:500 (anti-DIG, Roche #11333089001; anti-FITC, ThermoFisher #A889) at 4 °C overnight. The next day, embryos were washed in PBT (three quick washes followed by four 15-min washes), and then incubated at room temperature in blocking solution + secondary antibodies diluted 1:500 (AlexaFluor 488 and 555, ThermoFisher #A21206 and #A21436, respectively). After 2 hours, embryos were washed in PBT (three quick washes followed by four 15-min washes), mounted on Prolong Gold with DAPI (ThermoFisher, P36935) and left to curate overnight before imaging.

*Immunofluorescence*: embryos stored in methanol were washed in PBT (three quick washes followed by four 15-min washes), then in blocking solution for 30 min (Roche #11921673001; diluted 1:5 in PBT), before incubated overnight at 4 °C in blocking solution + primary antibody diluted 1:500 (mouse anti-beta galactosidase, Promega #Z378). The next day, embryos were washed in PBT (three quick washes followed by four 15-min washes), and then incubated at room temperature in blocking solution + secondary antibody (donkey anti-mouse AlexaFluor 555, ThermoFisher #A31570). After 2 hours, embryos were washed in PBT (three quick washes followed by four 15-min washes), mounted on Prolong Gold with DAPI (ThermoFisher, P36935) and left to curate overnight before imaging.

*Microscopy and data analysis*: embryos were imaged using a confocal microscope Zeiss LSM 880 confocal. Images were processed using a combination of automated scripts with manual curation. For 3D plots showing signal intensity across three regions of the embryo (Fig. 11, 2k, 3g, 5i), images were analyzed in ImageJ: a circular ROI of constant size was used to measure average intensity across the different regions (selected as shown in figures); number of lines/embryos analysed for each case are indicated in figure legends. For analyzing *E3N* mutant lines (Fuqua et al., 2021), individual nuclei were identified using the automated threshold algorithm on ImageJ and a watershed to split large ROIs; average intensities for each nucleus were measured. For analyzing *eveS2* mutant lines, we used ImageJ to perform Z-projections of max intensity, and a MATLAB (version R2018b; The MathWorks, Inc.) automated image analysis pipeline (named *Script-GAC*) was developed to capture expression signal along the AP axis on stage 5 embryos. For automated rotation, an ellipse was fitted on a masked embryo, and embryos were rotated based on the maximum Feret diameter. For quantification, a section with 30% of the height of the embryo was taken at a middle position and along the AP axis of each embryo. From this image section, the intensities from all the rows in the image matrix were averaged for each pixel position along the AP axis. The integration and analysis from each of these resultant AP embryo expression profiles were done in R (R Core Team, 2021). These expression profiles were smoothed with a Gaussian filter and then a linear interpolation was performed in order to have fixed samples number for the AP axis. Background removal and normalization were done based on the 10% and 50% quantile intensities, respectively, from the last 20% of the egg length. All embryos expression profiles per each genetic line were bootstrapped in order to see their reporter expression distribution along the AP axis. The bootstrapping was done using a confidence interval of 95% with 1000 replicates. For analyzing *twiPE* mutant lines, we used ImageJ to perform background subtraction from Z-projections of max intensity, rotate embryos to a vertical position and select a ROI at a defined position based on the intersection between 50% of the embryo long axis and the border of the *snail* RNA signal. We then used MorphoLibJ plugin in ImageJ to mask nuclei (volume higher than 3) and extracted intensities. For analyzing *rhoNEE* mutant lines, we used a custom code written in MATLAB (version R2018b; The MathWorks, Inc.), named *Script-MLP*; briefly, individual nuclei were segmented from the DAPI channel using a subroutine from the LivemRNA software package (Garcia et al., 2013). Stripes were then automatically identified by the following procedure: (1) bin nuclei by anterior-posterior (AP) coordinate; (2) within each bin, calculate a smoothed fluorescence profile along the dorsoventral (DV) coordinate based on the average fluorescence of each nucleus and its DV position; (3) identify peaks in the fluorescence

profile for each bin; (4) align peaks across bins. Within each bin, nuclei falling within the AP coordinates for the half maximum height of a peak (on either side) were automatically considered to belong to the corresponding stripe. Manual curation was applied to fix any errors in stripe identification. Each stripe was then fitted lengthwise (AP axis) with a piecewise linear function through the middle, where for each line segment the stripe width was calculated perpendicular to the segment as the largest distance between the centers of nuclei “belonging” to the segment (i.e., nuclei with AP position falling between the AP coordinates of the two ends of the segment). Overall stripe width was calculated as the average of the widths of constituent segments. For analyzing *tinB* mutant lines, Z-projections of max intensity were generated using ImageJ and then embryos rotated and cropped to the minimum size in which the entire embryo still fitted the image. Composite images were then concatenated together and a montage was made using a scale factor of 1.0. Next, nuclear intensities were measured for each embryo in the montage. Channels were split, and in the DAPI channel the montage was smoothed twice. A threshold was manually set and applied, after which we used the “analyze particles” function based on a selection range of 100 to infinity. This threshold range was overlaid with the reporter channel, and nuclear intensities per embryo were retrieved using the ROI Manager.

#### Motif prediction analysis of random sequences

Position weight matrices (PWMs) for *Drosophila melanogaster* and their logos were obtained from FlyFactorSurvey (Zhu et al., 2011). PWMs for specific stages of fly development were retrieved from (Li and Wunderlich, 2017). Motif search analysis was done using FIMO (Grant et al., 2011) and setting a threshold p-value of 0.001. The top 30% highest PWM-scores were selected to explore putative candidates for TFs binding sites.

#### Information content

Information content for each of the TF motifs can be estimated using the Kullback-Leibler distance:

$$I_{motif} = \sum_{i=1}^L \sum_{n=A}^T p_{i,n} \log_2 \left( \frac{p_{i,n}}{b_n} \right)$$

Where  $p_{i,n}$  is the probability of observing the nucleotide “n” at position “i” and  $b_n$  is the background frequency of nucleotide “n”. These values can be an indicative of how frequent a motif hit is expected by chance where  $2^{-I_{motif}}$  is an approximation of the probability for this event (Schneider et al., 1986). The empirical cumulative distribution plot for the information content scores was done in R.

## DATA AND CODE AVAILABILITY

All fly lines and resources will be made available from corresponding author upon reasonable request. Automated scripts used can be found attached to this paper.

## ACKNOWLEDGEMENTS

We thank GenScript for gifting us the random DNA libraries, Hsiao-Yun Liu for making the protein for the Zelda antibody prep, Garth Ilsley for discussions about pattern quantifications, Claire Standley for title suggestions and Denis Krndija for critical feedback on the manuscript. We are grateful to other members of the Crocker lab for helpful suggestions and discussions during the course of the project, in particular Xueying Li. We also thank the ALMF imaging platform and Alessandra Reversi for some of the fly injections. R.G. and L.G. are supported by fellowships from the European Molecular Biology Laboratory Interdisciplinary Postdoc Programme (EIPOD) under Marie Skłodowska-Curie Actions COFUND (664726 and 847543, respectively). Research in the Crocker lab is supported by the European Molecular Biology Laboratory (EMBL).

## AUTHOR CONTRIBUTIONS

Conceptualization: RG, TF, JC. Investigation: RG, GAC, MRPA, NB, TF, LG, NM, KR, EK, TK, CAR, JC. Methodology: RG, GAC, NB, TF, LG, KR, JC. Formal analysis: RG, GAC, NB, TF, LG, NM, JC. Data curation: RG, NM, JC. Visualization: RG, TF, KR, NM, JC. Software: GAC, MLP, JC. Resources: CAR. Supervision: RG, TF, JC. Project administration: RG, JC. Funding acquisition: JC. Writing, original draft: RG, JC. Writing, review & editing: RG, GAC, NB, TF, LG, NM, MRPA, MLP, JC.

## DECLARATION OF INTERESTS

The authors declare no competing interests.

## REFERENCES

Allan, D.W., and Thor, S. (2015). Transcriptional selectors, masters, and combinatorial codes: regulatory principles of neural subtype specification. Wiley Interdisciplinary Reviews: Developmental Biology 4, 505–528. <https://doi.org/10.1002/WDEV.191>.

de Almeida, B.P., Reiter, F., Pagani, M., and Stark, A. (2022). DeepSTARR predicts enhancer activity from DNA sequence and enables the *de novo* design of synthetic enhancers. Nat Genet 54, 613–624. <https://doi.org/10.1038/S41588-022-01048-5>.

Arnold, C.D., Gerlach, D., Spies, D., Matts, J.A., Sytnikova, Y.A., Pagani, M., Lau, N.C., and Stark, A. (2014). Quantitative genome-wide enhancer activity maps for five *Drosophila* species show functional enhancer conservation and turnover during *cis*-regulatory evolution. Nature Genetics 2014 46:7 46, 685–692. <https://doi.org/10.1038/ng.3009>.

Beerli, R.R., Segal, D.J., Dreier, B., and Barbas, C.F. (1998). Toward controlling gene expression at will: Specific regulation of the erbB-2/HER-2 promoter by using polydactyl zinc finger proteins constructed from modular building blocks. Proc Natl Acad Sci U S A 95, 14628–14633. <https://doi.org/10.1073/PNAS.95.25.14628>/ASSET/30887278-ED86-42C2-8C79-EA4D8AC5B98A/ASSETS/GRAPHIC/PQ2483845005.JPG.

Bier, E., Jan, L.Y., and Jan, Y.N. (1990). *rhomboid*, a gene required for dorsoventral axis establishment and peripheral nervous system development in *Drosophila melanogaster*. *Genes & Development* 4, 190–203. <https://doi.org/10.1101/GAD.4.2.190>.

Birnbaum, R.Y., Clowney, E.J., Agamy, O., Kim, M.J., Zhao, J., Yamanaka, T., Pappalardo, Z., Clarke, S.L., Wenger, A.M., Nguyen, L., et al. (2012). Coding exons function as tissue-specific enhancers of nearby genes. *Genome Research* 22, gr.133546.111. <https://doi.org/10.1101/GR.133546.111>.

de Boer, C.G., Vaishnav, E.D., Sadeh, R., Abeyta, E.L., Friedman, N., and Regev, A. (2019). Deciphering eukaryotic gene-regulatory logic with 100 million random promoters. *Nature Biotechnology* 2019 38:1 38, 56–65. <https://doi.org/10.1038/s41587-019-0315-8>.

Bourque, G., Leong, B., Vega, V.B., Chen, X., Yen, L.L., Srinivasan, K.G., Chew, J.L., Ruan, Y., Wei, C.L., Huck, H.N., et al. (2008). Evolution of the mammalian transcription factor binding repertoire via transposable elements. *Genome Research* 18, 1752. <https://doi.org/10.1101/GR.080663.108>.

Cande, J., Goltsev, Y., and Levine, M.S. (2009). Conservation of enhancer location in divergent insects. *Proc Natl Acad Sci U S A* 106, 14414–14419. [https://doi.org/10.1073/PNAS.0905754106/SUPPL\\_FILE/0905754106SI.PDF](https://doi.org/10.1073/PNAS.0905754106/SUPPL_FILE/0905754106SI.PDF).

Carroll, S.B. (2008). Evo-Devo and an Expanding Evolutionary Synthesis: A Genetic Theory of Morphological Evolution. *Cell* 134, 25–36. <https://doi.org/10.1016/J.CELL.2008.06.030>.

Chan, Y.F., Marks, M.E., Jones, F.C., Villarreal, G., Shapiro, M.D., Brady, S.D., Southwick, A.M., Absher, D.M., Grimwood, J., Schmutz, J., et al. (2010). Adaptive evolution of pelvic reduction in sticklebacks by recurrent deletion of a *pitxl* enhancer. *Science* (1979) 327, 302–305. [https://doi.org/10.1126/SCIENCE.1182213/SUPPL\\_FILE/CHAN-SOM.PDF](https://doi.org/10.1126/SCIENCE.1182213/SUPPL_FILE/CHAN-SOM.PDF).

Crocker, J., and Ilsley, G.R. (2017). Using synthetic biology to study gene regulatory evolution. *Current Opinion in Genetics & Development* 47, 91–101. <https://doi.org/10.1016/J.GDE.2017.09.001>.

Crocker, J., Noon, E.P.B., and Stern, D.L. (2015). The Soft Touch: Low-Affinity Transcription Factor Binding Sites in Development and Evolution. *Current Topics in Developmental Biology*.

Crocker, J., Ilsley, G.R., and Stern, D.L. (2016). Quantitatively predictable control of *Drosophila* transcriptional enhancers *in vivo* with engineered transcription factors. *Nature Genetics* 2016 48:3 48, 292–298. <https://doi.org/10.1038/ng.3509>.

Eichenlaub, M.P., and Ettwiller, L. (2011). De Novo Genesis of Enhancers in Vertebrates. *PLoS Biology* 9, 1001188. <https://doi.org/10.1371/JOURNAL.PBIO.1001188>.

Emera, D., and Wagner, G.P. (2012). Transposable element recruitments in the mammalian placenta: impacts and mechanisms. *Briefings in Functional Genomics* 11, 267–276. <https://doi.org/10.1093/BFGP/ELS013>.

Emera, D., Yin, J., Reilly, S.K., Gockley, J., and Noonan, J.P. (2016). Origin and evolution of developmental enhancers in the mammalian neocortex. *Proceedings of the National Academy of Sciences* *113*, E2617–E2626. <https://doi.org/10.1073/PNAS.1603718113>.

Erwin, D.H., and Davidson, E.H. (2009). The evolution of hierarchical gene regulatory networks. *Nature Reviews Genetics* *2009* *10*, 141–148. <https://doi.org/10.1038/nrg2499>.

Feschotte, C. (2008). Transposable elements and the evolution of regulatory networks. *Nature Reviews Genetics* *2008* *9*, 397–405. <https://doi.org/10.1038/nrg2337>.

Fong, S.L., and Capra, J.A. (2022). Function and constraint in enhancers with multiple evolutionary origins. *BioRxiv* *2022.01.05.475150*. <https://doi.org/10.1101/2022.01.05.475150>.

Foo, S.M., Sun, Y., Lim, B., Ziukaite, R., O'Brien, K., Nien, C.Y., Kirov, N., Shvartsman, S.Y., and Rushlow, C.A. (2014). Zelda potentiates morphogen activity by increasing chromatin accessibility. *Current Biology* *24*, 1341–1346. [https://doi.org/10.1016/J.CUB.2014.04.032/ATTACHMENT/0700DFB5-3541-4A18-97D3-0BCF4174E8E1/MMC1.PDF](https://doi.org/10.1016/J.CUB.2014.04.032).

Frankel, N., Davis, G.K., Vargas, D., Wang, S., Payre, F., and Stern, D.L. (2010). Phenotypic robustness conferred by apparently redundant transcriptional enhancers. *Nature* *2010* *466*:7305 *466*, 490–493. <https://doi.org/10.1038/nature09158>.

Frankel, N.S., Ereyilmaz, D.F., McGregor, A.P., Wang, S., Payre, F., and Stern, D.L. (2011). Morphological evolution caused by many subtle-effect substitutions in regulatory DNA. *Nature* *2011* *474*:7353 *474*, 598–603. <https://doi.org/10.1038/nature10200>.

Fuqua, T., Jordan, J., van Breugel, M.E., Halavatyi, A., Tischer, C., Polidoro, P., Abe, N., Tsai, A., Mann, R.S., Stern, D.L., et al. (2020). Dense and pleiotropic regulatory information in a developmental enhancer. *Nature* *587*, 235–239. <https://doi.org/10.1038/s41586-020-2816-5>.

Fuqua, T., Jordan, J., Halavatyi, A., Tischer, C., Richter, K., and Crocker, J. (2021). An open-source semi-automated robotics pipeline for embryo immunohistochemistry. *Scientific Reports* *2021* *11*:1 *11*, 1–16. <https://doi.org/10.1038/s41598-021-89676-5>.

Galupa, R., and Heard, E. (2017). Topologically Associating Domains in Chromosome Architecture and Gene Regulatory Landscapes during Development, Disease, and Evolution. *Cold Spring Harbor Symposia on Quantitative Biology* *82*, 267–278. <https://doi.org/10.1101/sqb.2017.82.035030>.

Garcia, H.G., Tikhonov, M., Lin, A., and Gregor, T. (2013). Quantitative Imaging of Transcription in Living Drosophila Embryos Links Polymerase Activity to Patterning. *Current Biology* *23*, 2140–2145. <https://doi.org/10.1016/J.CUB.2013.08.054>.

Gilbertson, S.E., Walter, H.C., Gardner, K., Wren, S.N., Vahedi, G., and Weinmann, A.S. (2022). Topologically associating domains are disrupted by evolutionary genome rearrangements forming species-specific enhancer connections in mice and humans. *Cell Reports* *39*, 110769. <https://doi.org/10.1016/J.CELREP.2022.110769>.

Gompel, N., Prud'Homme, B., Wittkopp, P.J., Kassner, V.A., and Carroll, S.B. (2005). Chance caught on the wing: cis-regulatory evolution and the origin of pigment patterns in *Drosophila*. *Nature* 2005 **433**:7025 433, 481–487. <https://doi.org/10.1038/nature03235>.

Gophna, U. (2018). The unbearable ease of expression—how avoidance of spurious transcription can shape G+C content in bacterial genomes. *FEMS Microbiology Letters* 365, 267. <https://doi.org/10.1093/FEMSLE/FNY267>.

Grant, C.E., Bailey, T.L., and Noble, W.S. (2011). FIMO: scanning for occurrences of a given motif. *Bioinformatics* 27, 1017–1018. <https://doi.org/10.1093/BIOINFORMATICS/BTR064>.

Guerreiro, I., Nunes, A., Woltering, J.M., Casaca, A., Nóvoa, A., Vinagre, T., Hunter, M.E., Duboule, D., and Mallo, M. (2013). Role of a polymorphism in a Hox/Pax-responsive enhancer in the evolution of the vertebrate spine. *Proc Natl Acad Sci U S A* 110, 10682–10686. [https://doi.org/10.1073/PNAS.1300592110/SUPPL\\_FILE/PNAS.201300592SI.PDF](https://doi.org/10.1073/PNAS.1300592110/SUPPL_FILE/PNAS.201300592SI.PDF).

Halfon, M.S. (2019). Studying Transcriptional Enhancers: The Founder Fallacy, Validation Creep, and Other Biases. *Trends in Genetics* 35, 93–103. <https://doi.org/10.1016/J.TIG.2018.11.004>.

Hansen, J.L., Loell, K.J., and Cohen, B.A. (2022). The Pioneer Factor Hypothesis is not necessary to explain ectopic liver gene activation. *Elife* 11. <https://doi.org/10.7554/ELIFE.73358>.

Hare, E.E., Peterson, B.K., Iyer, V.N., Meier, R., and Eisen, M.B. (2008). Sepsid even-skipped Enhancers Are Functionally Conserved in *Drosophila* Despite Lack of Sequence Conservation. *PLOS Genetics* 4, e1000106. <https://doi.org/10.1371/JOURNAL.PGEN.1000106>.

Harrison, M.M., Li, X.Y., Kaplan, T., Botchan, M.R., and Eisen, M.B. (2011). Zelda Binding in the Early *Drosophila melanogaster* Embryo Marks Regions Subsequently Activated at the Maternal-to-Zygotic Transition. *PLOS Genetics* 7, e1002266. <https://doi.org/10.1371/JOURNAL.PGEN.1002266>.

Indjeian, V.B., Kingman, G.A., Jones, F.C., Guenther, C.A., Grimwood, J., Schmutz, J., Myers, R.M., and Kingsley, D.M. (2016). Evolving New Skeletal Traits by cis-Regulatory Changes in Bone Morphogenetic Proteins. *Cell* 164, 45–56. <https://doi.org/10.1016/J.CELL.2015.12.007>.

Ip, Y.T., Park, R.E., Kosman, D., Bier, E., and Levine, M. (1992). The dorsal gradient morphogen regulates stripes of rhomboid expression in the presumptive neuroectoderm of the *Drosophila* embryo. *Genes & Development* 6, 1728–1739. <https://doi.org/10.1101/GAD.6.9.1728>.

Iwafuchi-Doi, M. (2019). The mechanistic basis for chromatin regulation by pioneer transcription factors. *Wiley Interdiscip. Rev. Syst. Biol. Med.* 11, e1427..

Jacobs, J., Atkins, M., Davie, K., Imrichova, H., Romanelli, L., Christiaens, V., Hulselmans, G., Potier, D., Wouters, J., Taskiran, I.I., et al. (2018). The transcription factor Grainy head

primes epithelial enhancers for spatiotemporal activation by displacing nucleosomes. *Nature Genetics* 2018 50:7 50, 1011–1020. <https://doi.org/10.1038/s41588-018-0140-x>.

Jiang, J., Kosman, D., Ip, Y.T., and Levine, M. (1991). The dorsal morphogen gradient regulates the mesoderm determinant twist in early *Drosophila* embryos. *Genes & Development* 5, 1881–1891. <https://doi.org/10.1101/GAD.5.10.1881>.

Jindal, G.A., and Farley, E.K. (2021). Enhancer grammar in development, evolution, and disease: dependencies and interplay. *Developmental Cell* 56, 575–587. <https://doi.org/10.1016/J.DEVCEL.2021.02.016>.

Kakidani, H., and Ptashne, M. (1988). GAL4 activates gene expression in mammalian cells. *Cell* 52, 161–167. [https://doi.org/10.1016/0092-8674\(88\)90504-1](https://doi.org/10.1016/0092-8674(88)90504-1).

Klemm, S.L., Shipony, Z., and Greenleaf, W.J. (2019). Chromatin accessibility and the regulatory epigenome. *Nature Reviews Genetics* 2018 20:4 20, 207–220. <https://doi.org/10.1038/s41576-018-0089-8>.

Konishi, S., Izawa, T., Lin, S.Y., Ebana, K., Fukuta, Y., Sasaki, T., and Yano, M. (2006). An SNP caused loss of seed shattering during rice domestication. *Science* (1979) 312, 1392–1396. [https://doi.org/10.1126/SCIENCE.1126410/SUPPL\\_FILE/KONISHI\\_SOM.PDF](https://doi.org/10.1126/SCIENCE.1126410/SUPPL_FILE/KONISHI_SOM.PDF).

Koshikawa, S. (2015). Enhancer modularity and the evolution of new traits. *Fly (Austin)* 9, 155–159. <https://doi.org/10.1080/19336934.2016.1151129>.

Koshikawa, S., Giorgianni, M.W., Vaccaro, K., Kassner, V.A., Yoder, J.H., Werner, T., and Carroll, S.B. (2015). Gain of cis-regulatory activities underlies novel domains of wingless gene expression in *Drosophila*. *Proc Natl Acad Sci U S A* 112, 7524–7529. <https://doi.org/10.1073/PNAS.1509022112>.

Kvon, E.Z., Kazmar, T., Stampfel, G., Yáñez-Cuna, J.O., Pagani, M., Schernhuber, K., Dickson, B.J., and Stark, A. (2014). Genome-scale functional characterization of *Drosophila* developmental enhancers *in vivo*. *Nature* 2014 512:7512 512, 91–95. <https://doi.org/10.1038/nature13395>.

Kvon, E.Z., Kamneva, O.K., Melo, U.S., Barozzi, I., Osterwalder, M., Mannion, B.J., Tissières, V., Pickle, C.S., Plajzer-Frick, I., Lee, E.A., et al. (2016). Progressive Loss of Function in a Limb Enhancer during Snake Evolution. *Cell* 167, 633-642.e11. <https://doi.org/10.1016/J.CELL.2016.09.028/ATTACHMENT/137E2323-216B-446E-869C-32653F4064C5/MMC1.PDF>.

Kvon, E.Z., Zhu, Y., Kelman, G., Novak, C.S., Plajzer-Frick, I., Kato, M., Garvin, T.H., Pham, Q., Harrington, A.N., Hunter, R.D., et al. (2020). Comprehensive In Vivo Interrogation Reveals Phenotypic Impact of Human Enhancer Variants. *Cell* 180, 1262. <https://doi.org/10.1016/J.CELL.2020.02.031>.

Kvon, E.Z., Waymack, R., Gad, M., and Wunderlich, Z. (2021). Enhancer redundancy in development and disease. *Nature Reviews Genetics* 2021 22:5 22, 324–336. <https://doi.org/10.1038/s41576-020-00311-x>.

Lack, J.B., Lange, J.D., Tang, A.D., Corbett-Detig, R.B., and Pool, J.E. (2016). A Thousand Fly Genomes: An Expanded *Drosophila* Genome Nexus. *Molecular Biology and Evolution* 33, 3308–3313. <https://doi.org/10.1093/MOLBEV/MSW195>.

Laland, K.N., Uller, T., Feldman, M.W., Sterelny, K., Müller, G.B., Moczek, A., Jablonka, E., and Odling-Smee, J. (2015). The extended evolutionary synthesis: its structure, assumptions and predictions. *Proceedings of the Royal Society B: Biological Sciences* 282. <https://doi.org/10.1098/RSPB.2015.1019>.

Larson, E.D., Komori, H., Gibson, T.J., Ostgaard, C.M., Hamm, D.C., Schnell, J.M., Lee, C.Y., and Harrison, M.M. (2021). Cell-type-specific chromatin occupancy by the pioneer factor Zelda drives key developmental transitions in *Drosophila*. *Nature Communications* 2021 12:1 12, 1–17. <https://doi.org/10.1038/s41467-021-27506-y>.

Li, L., and Wunderlich, Z. (2017). An enhancer's length and composition are shaped by its regulatory task. *Frontiers in Genetics* 8, 63. [https://doi.org/10.3389/FGENE.2017.00063/BIBTEX](https://doi.org/10.3389/FGENE.2017.00063).

Li, S., Hannenhalli, S., and Ovcharenko, I. (2022). De novo human brain enhancers created by single nucleotide mutations. *BioRxiv* 2021.07.04.451055. <https://doi.org/10.1101/2021.07.04.451055>.

Lindhorst, D., and Halfon, M.S. (2022). Reporter gene assays and chromatin-level assays define substantially non-overlapping sets of enhancer sequences. *BioRxiv* 2022.04.21.489091. <https://doi.org/10.1101/2022.04.21.489091>.

Loker, R., Sanner, J.E., and Mann, R.S. (2021). Cell-type-specific Hox regulatory strategies orchestrate tissue identity. *Current Biology* 31, 4246–4255.e4. <https://doi.org/10.1016/J.CUB.2021.07.030>.

Long, H.K., Prescott, S.L., and Wysocka, J. (2016). Ever-Changing Landscapes: Transcriptional Enhancers in Development and Evolution. *Cell* 167, 1170–1187. <https://doi.org/10.1016/J.CELL.2016.09.018>.

López-Rivera, F., Foster Rhoades, O.K., Vincent, B.J., Pym, E.C.G., Bragdon, M.D.J., Estrada, J., DePace, A.H., and Wunderlich, Z. (2020). A Mutation in the *Drosophila melanogaster* eve Stripe 2 Minimal Enhancer Is Buffered by Flanking Sequences. *G3 Genes|Genomes|Genetics* 10, 4473–4482. <https://doi.org/10.1534/G3.120.401777>.

Lupiáñez, D.G., Spielmann, M., and Mundlos, S. (2016). Breaking TADs: How Alterations of Chromatin Domains Result in Disease. *Trends in Genetics* 32, 225–237. <https://doi.org/10.1016/j.tig.2016.01.003>.

Lynch, V.J., Leclerc, R.D., May, G., and Wagner, G.P. (2011). Transposon-mediated rewiring of gene regulatory networks contributed to the evolution of pregnancy in mammals. *Nature Genetics* 2011 43:11 43, 1154–1159. <https://doi.org/10.1038/ng.917>.

Majic, P., and Payne, J.L. (2020). Enhancers Facilitate the Birth of De Novo Genes and Gene Integration into Regulatory Networks. *Molecular Biology and Evolution* 37, 1165–1178. <https://doi.org/10.1093/MOLBEV/MSZ300>.

Markstein, M., Zinzen, R., Markstein, P., Yee, K.-P., Erives, A., Stathopoulos, A., and Levine, M. (2004). A regulatory code for neurogenic gene expression in the *Drosophila* embryo. *Development* *131*, 2387–2394. <https://doi.org/10.1242/DEV.01124>.

Monroe, J.G., Srikant, T., Carbonell-Bejerano, P., Becker, C., Lensink, M., Exposito-Alonso, M., Klein, M., Hildebrandt, J., Neumann, M., Kliebenstein, D., et al. (2022). Mutation bias reflects natural selection in *Arabidopsis thaliana*. *Nature* *2022* *602*:7895 *602*, 101–105. <https://doi.org/10.1038/s41586-021-04269-6>.

Monteiro, A., and Gupta, M.D. (2016). Identifying Coopted Networks and Causative Mutations in the Origin of Novel Complex Traits. *Current Topics in Developmental Biology* *119*, 205–226. <https://doi.org/10.1016/BS.CTDB.2016.03.003>.

Muers, M. (2013). Evolutionary insights into nucleosomes. *Nature Reviews Genetics* *2013* *14*: 79–79. <https://doi.org/10.1038/nrg3412>.

Nevil, M., Gibson, T.J., Bartolutti, C., Iyengar, A., and Harrison, M.M. (2020). Establishment of chromatin accessibility by the conserved transcription factor *Grainy head* is developmentally regulated. *Development (Cambridge)* *147*. <https://doi.org/10.1242/DEV.185009/VIDEO-1>.

Nghe, P., de Vos, M.G.J., Kingma, E., Kogenaru, M., Poelwijk, F.J., Laan, L., and Tans, S.J. (2020). Predicting Evolution Using Regulatory Architecture. [Https://Doi.Org/10.1146/Annurev-Biophys-070317-032939](https://doi.org/10.1146/Annurev-Biophys-070317-032939) *49*, 181–197. <https://doi.org/10.1146/ANNUREV-BIOPHYS-070317-032939>.

Oliver, K.R., and Greene, W.K. (2009). Transposable elements: powerful facilitators of evolution. *BioEssays* *31*, 703–714. <https://doi.org/10.1002/BIES.200800219>.

Pan, D.J., Huang, J.D., and Courey, A.J. (1991). Functional analysis of the *Drosophila* *twist* promoter reveals a dorsal-binding ventral activator region. *Genes & Development* *5*, 1892–1901. <https://doi.org/10.1101/GAD.5.10.1892>.

Peng, P.C., Khoueiry, P., Girardot, C., Reddington, J.P., Garfield, D.A., Furlong, E.E.M., and Sinha, S. (2019). The Role of Chromatin Accessibility in *cis*-Regulatory Evolution. *Genome Biology and Evolution* *11*, 1813–1828. <https://doi.org/10.1093/GBE/EVZ103>.

Le Poul, Y., Xin, Y., Ling, L., Mühling, B., Jaenichen, R., Hörl, D., Bunk, D., Harz, H., Leonhardt, H., Wang, Y., et al. (2020). Regulatory encoding of quantitative variation in spatial activity of a *Drosophila* enhancer. *Science Advances* *6*. [https://doi.org/10.1126/SCIADV.ABE2955/SUPPL\\_FILE/ABE2955\\_SM.PDF](https://doi.org/10.1126/SCIADV.ABE2955/SUPPL_FILE/ABE2955_SM.PDF).

Prabhakar, S., Visel, A., Akiyama, J.A., Shoukry, M., Lewis, K.D., Holt, A., Plajzer-Frick, I., Morrison, H., FitzPatrick, D.R., Afzal, V., et al. (2008). Human-specific gain of function in a developmental enhancer. *Science (1979)* *321*, 1346–1350. [https://doi.org/10.1126/SCIENCE.1159974/SUPPL\\_FILE/PRABHAKAR.SOM.PDF](https://doi.org/10.1126/SCIENCE.1159974/SUPPL_FILE/PRABHAKAR.SOM.PDF).

Preger-Ben Noon, E., Sabarís, G., Ortiz, D.M., Sager, J., Liebowitz, A., Stern, D.L., and Frankel, N. (2018). Comprehensive Analysis of a *cis*-Regulatory Region Reveals Pleiotropy in Enhancer Function. *Cell Reports* *22*, 3021–3031.

<https://doi.org/10.1016/J.CELREP.2018.02.073/ATTACHMENT/ED98C950-B7BF-42E6-A752-502C4B413A30/MMC1.PDF>.

R Core Team (2021). R: A language and environment for statistical computing.

Rebeiz, M., Pool, J.E., Kassner, V.A., Aquadro, C.F., and Carroll, S.B. (2009). Stepwise modification of a modular enhancer underlies adaptation in a *Drosophila* population. *Science* (1979) 326, 1663–1667.

[https://doi.org/10.1126/SCIENCE.1178357/SUPPL\\_FILE/REBEIZ.SOM.PDF](https://doi.org/10.1126/SCIENCE.1178357/SUPPL_FILE/REBEIZ.SOM.PDF).

Rebeiz, M., Jikomes, N., Kassner, V.A., and Carroll, S.B. (2011). Evolutionary origin of a novel gene expression pattern through co-option of the latent activities of existing regulatory sequences. *Proc Natl Acad Sci U S A* 108, 10036–10043.

[https://doi.org/10.1073/PNAS.1105937108/SUPPL\\_FILE/SAPP.PDF](https://doi.org/10.1073/PNAS.1105937108/SUPPL_FILE/SAPP.PDF).

Schneider, T.D., Stormo, G.D., Gold, L., and Ehrenfeucht, A. (1986). Information content of binding sites on nucleotide sequences. *Journal of Molecular Biology* 188, 415–431.

[https://doi.org/10.1016/0022-2836\(86\)90165-8](https://doi.org/10.1016/0022-2836(86)90165-8).

Schulz, K.N., Bondra, E.R., Moshe, A., Villalta, J.E., Lieb, J.D., Kaplan, T., McKay, D.J., and Harrison, M.M. (2015). *Zelda* is differentially required for chromatin accessibility, transcription factor binding, and gene expression in the early *Drosophila* embryo. *Genome Research* 25, 1715–1726. <https://doi.org/10.1101/GR.192682.115>.

Slattery, M., Riley, T., Liu, P., Abe, N., Gomez-Alcalá, P., Dror, I., Zhou, T., Rohs, R., Honig, B., Bussemaker, H.J., et al. (2011). Cofactor binding evokes latent differences in DNA binding specificity between *HOX* proteins. *Cell* 147, 1270–1282.

<https://doi.org/10.1016/J.CELL.2011.10.053/ATTACHMENT/92F95178-2BE1-4C53-941A-9AB57860E0ED/MMC1.PDF>.

Small, S., Kraut, R., Hoey, T., Warrior, R., and Levine, M. (1991). Transcriptional regulation of a pair-rule stripe in *Drosophila*. *Genes & Development* 5, 827–839.

<https://doi.org/10.1101/GAD.5.5.827>.

Small, S., Blair, A., and Levine, M. (1992). Regulation of even-skipped stripe 2 in the *Drosophila* embryo. *The EMBO Journal* 11, 4047–4057. <https://doi.org/10.1002/J.1460-2075.1992.TB05498.X>.

Smith, R.P., Riesenfeld, S.J., Holloway, A.K., Li, Q., Murphy, K.K., Feliciano, N.M., Orecchia, L., Oksenborg, N., Pollard, K.S., and Ahituv, N. (2013). A compact, *in vivo* screen of all 6-mers reveals drivers of tissue-specific expression and guides synthetic regulatory element design. *Genome Biology* 14, 1–15. <https://doi.org/10.1186/GB-2013-14-7-R72/COMMENTS>.

Song, Y., Park, J.O., Tanner, L., Nagano, Y., Rabinowitz, J.D., and Shvartsman, S.Y. (2019). Energy budget of *Drosophila* embryogenesis. *Current Biology* 29, R566–R567. <https://doi.org/10.1016/J.CUB.2019.05.025>.

Stanojevic, D., Small, S., and Levine, M. (1991). Regulation of a Segmentation Stripe by Overlapping Activators and Repressors in the *Drosophila* Embryo. *Science* (1979) *254*, 1385–1387. <https://doi.org/10.1126/SCIENCE.1683715>.

Stern, D.L., and Orgogozo, V. (2008). The Loci of Evolution: How Predictable is Genetic Evolution? *Evolution; International Journal of Organic Evolution* *62*, 2155. <https://doi.org/10.1111/J.1558-5646.2008.00450.X>.

Sun, Y., Nien, C.Y., Chen, K., Liu, H.Y., Johnston, J., Zeitlinger, J., and Rushlow, C. (2015). Zelda overcomes the high intrinsic nucleosome barrier at enhancers during *Drosophila* zygotic genome activation. *Genome Research* *25*, 1703–1714. <https://doi.org/10.1101/GR.192542.115>.

Surkova, S., Golubkova, E., Mamon, L., and Samsonova, M. (2018). Dynamic maternal gradients and morphogenetic networks in *Drosophila* early embryo. *Biosystems* *173*, 207–213. <https://doi.org/10.1016/J.BIOSYSTEMS.2018.10.009>.

Thisse, C., Perrin-Schmitt, F., Stoetzel, C., and Thisse, B. (1991). Sequence-specific transactivation of the *Drosophila* twist gene by the dorsal gene product. *Cell* *65*, 1191–1201. [https://doi.org/10.1016/0092-8674\(91\)90014-P](https://doi.org/10.1016/0092-8674(91)90014-P).

Vaishnav, E.D., de Boer, C.G., Molinet, J., Yassour, M., Fan, L., Adiconis, X., Thompson, D.A., Levin, J.Z., Cubillos, F.A., and Regev, A. (2022). The evolution, evolvability and engineering of gene regulatory DNA. *Nature* *2022* *603*:7901 *603*, 455–463. <https://doi.org/10.1038/s41586-022-04506-6>.

Vincent, B.J., Estrada, J., and DePace, A.H. (2016). The appeasement of Doug: a synthetic approach to enhancer biology. *Integrative Biology (United Kingdom)* *8*, 475–484. <https://doi.org/10.1039/c5ib00321k>.

Wade, J.T., and Grainger, D.C. (2018). Spurious transcription and its impact on cell function. *Transcription* *9*, 182. <https://doi.org/10.1080/21541264.2017.1381794>.

Webster, N., Jin, J.R., Green, S., Hollis, M., and Chambon, P. (1988). The yeast UASG is a transcriptional enhancer in human hela cells in the presence of the GAL4 trans-activator. *Cell* *52*, 169–178. [https://doi.org/10.1016/0092-8674\(88\)90505-3](https://doi.org/10.1016/0092-8674(88)90505-3).

Wunderlich, Z., and Mirny, L.A. (2009). Different gene regulation strategies revealed by analysis of binding motifs. *Trends in Genetics* *25*, 434–440. <https://doi.org/10.1016/J.TIG.2009.08.003>.

Xin, Y., le Poul, Y., Ling, L., Museridze, M., Mühling, B., Jaenichen, R., Osipova, E., and Gompel, N. (2020). Enhancer evolutionary co-option through shared chromatin accessibility input. *Proc Natl Acad Sci U S A* *117*, 20636–20644. <https://doi.org/10.1073/PNAS.2004003117>.

Yin, Z., Xu, X.L., and Frasch, M. (1997). Regulation of the twist target gene tinman by modular cis-regulatory elements during early mesoderm development. *Development* *124*, 4971–4982. <https://doi.org/10.1242/DEV.124.24.4971>.

Yona, A.H., Alm, E.J., and Gore, J. (2018). Random sequences rapidly evolve into de novo promoters. *Nature Communications* 2018 9:1 9, 1–10. <https://doi.org/10.1038/s41467-018-04026-w>.

Zaffran, S., Reim, I., Qian, L., Lo, P.C., Bodmer, R., and Frasch, M. (2006). Cardioblast-intrinsic Tinman activity controls proper diversification and differentiation of myocardial cells in *Drosophila*. *Development* 133, 4073–4083. <https://doi.org/10.1242/DEV.02586>.

Zaret, K.S., and Carroll, J.S. (2011). Pioneer transcription factors: establishing competence for gene expression. *Genes & Development* 25, 2227–2241.  
<https://doi.org/10.1101/GAD.176826.111>.

Zhu, L.J., Christensen, R.G., Kazemian, M., Hull, C.J., Enuameh, M.S., Basciotta, M.D., Brasefield, J.A., Zhu, C., Asriyan, Y., Lapointe, D.S., et al. (2011). FlyFactorSurvey: a database of *Drosophila* transcription factor binding specificities determined using the bacterial one-hybrid system. *Nucleic Acids Research* 39, D111–D117.  
<https://doi.org/10.1093/NAR/GKQ858>.